

OCCURRENCES OF FOITITE AND ROSSMANITE FROM THE KOKTOKAY NO. 3 GRANITIC PEGMATITE DYKE, ALTAI, NORTHWESTERN CHINA: A RECORD OF HYDROTHERMAL FLUIDS

AI CHENG ZHANG, RU CHENG WANG[§], HUAN HU and XIAO MING CHEN

*State Key Laboratory for Mineral Deposits Research and Department of Earth Sciences,
Nanjing University, Nanjing 210093, People's Republic of China*

HUI ZHANG

Institute of Geochemistry, Chinese Academy of Sciences, Guiyang 550002, People's Republic of China

ABSTRACT

Two species of X-site-vacant tourmalines, foitite and rossmanite, occur in the Koktokay No. 3 granitic pegmatite dyke, Altai, northwestern China, a spodumene-subtype pegmatite. Foitite–schorl crystals develop as fillings in the interstices among Fe-rich dravite crystals in the endocontact zone between the pegmatite dyke and the metagabbro country-rock. The evolution of the tourmaline crystals in the endocontact zone occurred in two stages. The first stage is typified by the formation of Fe-rich dravite with variable compositions described by substitutions $^X\text{Na}^{Y+Z}\text{R}(\square^{Y+Z}\text{Al})_{-1}$, $^{Y+Z}\text{ROH}(\text{AlO})_{-1}$, and $^X\text{Ca}^{Y+Z}\text{R}_2(\square^{Y+Z}\text{Al}_2)_{-1}$ (where $^{Y+Z}\text{R} = \text{Fe}_{\text{tot}} + \text{Mg} + \text{Mn} + \text{Zn}$). The second-stage foitite–schorl has compositional variations expressed by $\text{Fe}(\text{Mg})_{-1}$, $^X\text{Na}^{Y+Z}\text{R}(\square^{Y+Z}\text{Al})_{-1}$, $^{Y+Z}\text{ROH}(\text{AlO})_{-1}$, and less $^X\text{Ca}^{Y+Z}\text{R}_2(\square^{Y+Z}\text{Al}_2)_{-1}$. Dravite may develop as a result of pegmatite-derived fluids reacting with fluids from the country rock, whereas the formation of foitite–schorl is mainly attributed to pegmatite-derived fluids, the occurrence of foitite further reflecting the low Ca and Na concentrations in the fluids. In the “cleavelandite”–spodumene zone, rossmanite occurs as veinlets within the main mass of elbaite crystals and exhibits a preferred orientation, and its compositional variation also can be described in two stages. In the first stage, the compositional variations of elbaite can be described by the substitution $^X\square^Y\text{Al}[\text{Na}^Y(\text{Fe},\text{Mn})]_{-1}$, whereas in the second stage, the minor compositional variation of rossmanite can be expressed by the substitution $^Y\text{AlO}_2[\text{Li}(\text{OH})_2]_{-1}$. The high X-site vacancy in elbaite may be caused by the buffering effect of a Na-rich phase, whereas the formation of rossmanite is most likely controlled by the local lack of Na and Ca in the late hydrothermal fluids.

Keywords: foitite, rossmanite, tourmaline, granitic pegmatite, Koktokay No. 3 dyke, Altai, China.

SOMMAIRE

Deux espèces de tourmaline contenant des lacunes au site X, la foïtite et la rossmanite, se trouvent dans le filon de pegmatite granitique de Koktokay No. 3, région de l'Altaï, dans le secteur nord-ouest de la Chine. Des cristaux de foïtite–schorl remplissent les interstices parmi les cristaux de dravite ferrière dans la zone endocontact entre cette pegmatite à spodumène et l'encaissant métagabbroïque. L'évolution de ces cristaux de tourmaline a eu lieu en deux étapes. La première a impliqué la formation de dravite ferrière avec des compositions variables décrites selon les schémas de substitution suivants: $^X\text{Na}^{Y+Z}\text{R}(\square^{Y+Z}\text{Al})_{-1}$, $^{Y+Z}\text{ROH}(\text{AlO})_{-1}$, et $^X\text{Ca}^{Y+Z}\text{R}_2(\square^{Y+Z}\text{Al}_2)_{-1}$ (dans lesquels $^{Y+Z}\text{R} = \text{Fe}_{\text{tot}} + \text{Mg} + \text{Mn} + \text{Zn}$). La foïtite–schorl du second stade montre des compositions variant selon $\text{Fe}(\text{Mg})_{-1}$, $^X\text{Na}^{Y+Z}\text{R}(\square^{Y+Z}\text{Al})_{-1}$, $^{Y+Z}\text{ROH}(\text{AlO})_{-1}$ et, à un degré moindre, $^X\text{Ca}^{Y+Z}\text{R}_2(\square^{Y+Z}\text{Al}_2)_{-1}$. La dravite semble s'être développée à partir de fluides dérivés de la pegmatite, en réaction avec des fluides dérivés des roches encaissantes, tandis que la formation de la série foïtite–schorl serait plutôt attribuée à des fluides dérivés de la pegmatite, l'incidence de la foïtite étant plutôt due à la faible concentration du Ca et du Na dans la phase fluide. Dans la zone à “cleavelandite” – spodumène, la rossmanite se présente en veinules dans la masse principale d'elbaïte, et fait preuve d'une orientation préférentielle. La variation dans sa composition serait aussi due à deux stades. Au premier, les variations en composition de l'elbaïte sont attribuables au schéma de substitution $^X\square^Y\text{Al}[\text{Na}^Y(\text{Fe},\text{Mn})]_{-1}$, tandis qu'au second stade, les fluctuations mineures en composition de la rossmanite seraient régies par le schéma de substitution $^Y\text{AlO}_2[\text{Li}(\text{OH})_2]_{-1}$. Le taux élevé de lacunes au site X de l'elbaïte pourrait résulter de l'effet tampon à cause d'une phase sodique coexistante, tandis que la formation de la rossmanite serait probablement due à une déficience locale en Na et Ca dans la phase fluide tardive.

(Traduit par la Rédaction)

Mots-clés: foïtite, rossmanite, tourmaline, pegmatite granitique, filon Koktokay No. 3, Altaï, Chine.

[§] E-mail address: rcwang@nju.edu.cn

INTRODUCTION

Tourmaline has the general formula $XY_3Z_6[T_6O_{18}] [BO_3]_3V_3W$, where $X = Na, Ca, K, \text{vacancy } (X^{\square})$; $Y = Mg, Fe^{2+}, Mn^{2+}, Al, Fe^{3+}, Mn^{3+}, Li, V^{3+}, Ti^{4+}$; $Z = Al, Fe^{3+}, Cr^{3+}, Mg$; $T = Si, Al, B$; $V = OH, O$; and $W = OH, O$ and F (Hawthorne & Henry 1999). The complex composition of tourmaline leads to a wide variety of end members. On the basis of dominant species at the X site, Hawthorne & Henry (1999) divided tourmalines into three principal groups: alkali tourmalines, the most commonly encountered, calcic tourmalines and X -site-vacant tourmalines. So far, only four natural X -site-vacant end-members of tourmaline have been reported: foitite (MacDonald *et al.* 1993), rossmanite (Selway *et al.* 1998), magnesiofoitite (Hawthorne *et al.* 1999), and "oxy-foitite" (Medaris *et al.* 2003).

Foitite may be found as hair-like crystals in pockets of granitic pegmatites and some hydrothermally affected rocks (*e.g.*, Foit *et al.* 1989, Pezzotta *et al.* 1996, Aurisicchio *et al.* 1999, Francis *et al.* 1999, Novák & Taylor 2000, Medaris *et al.* 2003), and in some cases, it is described as the initial generation of fibrous tourmaline that replaces elbaite (*e.g.*, Dutrow & Henry 2000) and as the fibrous tourmaline of replacement origin in fractured pre-existing tourmaline (*e.g.*, Henry *et al.* 2002). However, magnesiofoitite has been reported in only two localities, the Sullivan Pb–Zn–Ag deposit, British Columbia (Jiang *et al.* 1997) and the Kyonosawa area, Japan (Hawthorne *et al.* 1999), and rossmanite has been described only at the type locality (Selway *et al.* 1998); recently, "oxy-foitite" was described from the Baraboo quartzite, Wisconsin (Medaris *et al.* 2003). Clearly, investigations of X -site-vacant tourmalines are rather limited. During a systematic examination of tourmaline from the Koktokay No. 3 granitic pegmatite dyke, Altai, northwestern China, we identified two X -site-vacant tourmalines, foitite and rossmanite, exhibiting various levels of X -site vacancy. Unlike previously reported examples, foitite appears as fillings in the interstices among dravite crystals in the endocontact zone of the Koktokay No. 3 granitic pegmatite dyke, whereas rossmanite appears as veinlets within the host elbaite crystals. Here, we report on the unusual occurrences and chemical characteristics of foitite and rossmanite, and their possible origins.

GEOLOGICAL SETTING OF THE KOKTOKAY No. 3
GRANITIC PEGMATITE DYKE

The Koktokay No. 3 granitic pegmatite dyke is one of thousands of pegmatite dykes in the Altai pegmatite district, northwestern China. According to the classification of Černý (1991), the Koktokay No. 3 granitic pegmatite dyke belongs to spodumene subtype of pegmatite. In the past several decades, it was mainly mined for spodumene, lepidolite, beryl, and columbite–tantalite.

The pegmatite dyke intruded metagabbro, and formed during the Yanshanian interval (177.9–148.0 Ma) (Chen *et al.* 1999). Between the pegmatite dyke and metagabbro, there exists a narrow contact zone several centimeters wide; an exocontact zone and an endocontact zone can be recognized. The exocontact zone, close to the metagabbro, mainly contains dravite and apatite, whereas the endocontact zone, close to the pegmatite dyke, mainly contains tourmaline, quartz, muscovite, and accessory albite and zircon. The overall shape of the pegmatite dyke looks like a solid cap, and consists of a gently dipping "plate" and a steeply dipping cupola protruding upward from the plate. The pegmatite dyke shows a well-developed internal textural zonation both in the "plate" and in the cupola. From the uppermost textural zone of the "plate" downward, the following seven mineralogical-textural zones can be distinguished: I Graphic pegmatite zone, II Blocky microcline zone, III Muscovite – quartz zone, IV Saccharoidal albite zone, V "Cleavelandite" – quartz – spodumene zone, VI Albite–lepidolite zone, and VII Fine-grained albite zone. However, from the outermost textural zone inward, the cupola contains the following nine mineralogical-textural zones: I Graphic pegmatite zone, II Saccharoidal albite zone, III Blocky microcline zone, IV Muscovite – quartz zone, V "Cleavelandite" – spodumene zone, VI Quartz – spodumene zone, VII Thinly bladed albite – muscovite zone, VIII Lepidolite – thinly bladed albite zone, IX Blocky quartz and microcline core (Zhu *et al.* 2000). Building on the results of Wang *et al.* (1981), Zhang *et al.* (2003) have established a list of associations of important minerals in the cupola of the Koktokay No. 3 granitic pegmatite dyke (Table 1).

TABLE 1. SUMMARY OF DISTRIBUTION OF ROCK-FORMING AND ACCESSORY MINERALS IN DIFFERENT ZONES OF THE CUPOLA, KOKTOKAY No. 3 GRANITIC PEGMATITE DYKE, ALTAI, NW CHINA

Texture zone	I	II	III	IV	V	VI	VII	VIII	IX
Microcline	43	50	77	21	1	1	2	1	49
Albite	17	33	7	8	51	22	63	31	
Quartz	31	10	13	54	30	85	15	2	48
Muscovite	6	4	2	15	5	4	12		1
Spodumene	+	+	+	+++	12	17	6	1	1
Lepidolite							+	64	
Beryl	++	+++	++	+++	++	++	++	++	+
Col–Tan	+	++	+	++	+++	++	++	++	+
Pollucite					+	++	+++	+++	++
Tapiolite									+
Uranmicrolite					+	+	++		
Zircon	+	+	+	+	++	+	++	+	+
Schorl	+	+	++	+++	++	+	+	+	+
Elbaite					+	+		++	
Fluorapatite	++	+++	++	+++	++	++	+++	+++	+
Sps–Alm	+++	+++	++	++	+	+	+	+	+
Montebrasite					++	+		+	
Triplite				+	++	++			
Thortite					+	+	+		

Relative abundances of rock-forming minerals were estimated in vol.%. The symbols +, ++ and +++ denote rare, present and abundant, respectively. Zones I to IX denote different textural zones. Symbols: Col–Tan: columbite–tantalite series, Sps–Alm: spessartine–almandine series.

OCCURRENCE OF FOITITE AND ROSSMANITE

Tourmaline occurs both in the contact zone and in most of the internal textural zones of the pegmatite dyke in the cupola. Tourmaline crystals from the contact zone and zones I to IV are black, whereas tourmaline crystals from zones V and VII are pink. In general, the size of tourmaline becomes larger from the contact zone to the core of the pegmatite. However, interestingly, the occurrences of X-site-vacant tourmalines are localized, with foitite–schorl restricted to the endocontact zone, and rossmanite restricted to the “cleavelandite” – spodumene zone.

The endocontact zone

The tourmaline in the endocontact zone is a bimodal mixture of dravite and foitite–schorl. The dravite crystals show intense pleochroism ranging from yellow to bluish green in thin section. Most of the elongate columnar dravite crystals are distributed perpendicular to the contact wall, and their sizes can be up to 3×10 mm. Some euhedral crystals of dravite and anhedral fragments are simply zoned, and the outer zones are commonly lighter than the inner zones in the back-scattered electron (BSE) images (Fig. 1a). Interestingly, unlike hair-like crystals described in the literature, the foitite–schorl crystals described here invariably develop as fillings in the interstices among the dravite crystals (Fig. 1a). The BSE image in Figure 1b reveals that the foitite–schorl crystals are also slightly heterogeneous; however, no obvious regularity in compositional heterogeneity was observed among different foitite–schorl crystals. Dravite and foitite–schorl are mainly associated with quartz, muscovite, plagioclase, apatite, and zircon.

The “cleavelandite” – spodumene zone

In the “cleavelandite” – spodumene zone, the 1×3 cm pink tourmaline crystals include elbaite and rossmanite, and they are colorless in thin section. The pink columnar crystals of elbaite are cross-cut by later veinlets of rossmanite (Fig. 2). The host crystals of elbaite exhibit a large variation in brightness in the BSE images (Fig. 2), indicating a variable composition. The rossmanite veinlets are generally several micrometers wide and exhibit a preferred orientation. Associated minerals include “cleavelandite”, spodumene, quartz, Nb–Ta oxides, and hafnian zircon.

ANALYTICAL METHODS

The chemical compositions of tourmaline were obtained with a JEOL JXA–8800M electron microprobe using wavelength-dispersion spectrometry (WDS) at the State Key Laboratory for Mineral Deposits Research, Nanjing University. The microprobe was operated at an

accelerating voltage of 15 kV and a sample current of 10 nA. The following standards were used: hornblende (Na, K, Mg, Si, Ca, Ti, and Fe), Durango fluorapatite (F), Amelia albite (Al), MnTiO₃ (Mn) and ZnO (Zn), and the detection limits (ppm) of some minor elements are: Ti 250, Fe 500, Mg 300, Mn 550, Zn 300, Ca 150, Na 350, K 130, and F 2500. Element peaks and backgrounds were measured for all elements with counting times of 10 s and 5 s, respectively. All data were reduced using the ZAF program.

Structural formulae were calculated on the basis of 31 anions (O, OH, F), assuming stoichiometric amounts of H₂O as (OH), *i.e.*, OH + F = 4 *apfu* (atoms per formula unit), B₂O₃ (3 *apfu* B) and Li₂O (as Li⁺). The amount of Li assigned to the Y site corresponds to the ideal sum of the cations occupying the T + Z + Y sites (15 *apfu*) minus the sum of the cations actually occupying these sites [Li = 15 – (Si + Al + Mg + Fe + Mn + Zn + Ti)]; the calculation was iterated to self-consistency. All Fe and Mn were assumed to be divalent. The nomenclature of Hawthorne & Henry (1999) is used in this paper. The structural formula calculations were performed by using the Microsoft Excel™ worksheet from the following web address: <http://tabitha.open.ac.uk/tindle/AGTHome.html>.

CHEMICAL COMPOSITIONS OF TOURMALINE

Dravite and foitite–schorl in the endocontact zone

Sixty-nine point-analyses of dravite and foitite–schorl in the endocontact zone were made, and representative results of analyses are given in Table 2, with the contents of the X-site cations plotted on the triangular diagram (Fig. 3). In the zoned crystals of dravite, Mg contents vary from 1.756 to 2.106 atoms per formula unit (*apfu*), whereas Fe contents range between 0.767 and 1.210 *apfu*. At the Y + Z sites, aluminum (^{Y+Z}Al) varies from 5.785 to 6.265 *apfu*. The Ti contents are low (0.058 *apfu* on average), whereas Ca and Na contents at the X site range from 0.161 to 0.344 *apfu* and from 0.405 to 0.559 *apfu*, respectively. As a consequence of variable X-site occupancies, the X-site vacancies vary from 0.114 to 0.420 *apfu* (Fig. 3). In general, zoned dravite displays core-to-rim variations in the Fe:Mg ratio (*e.g.*, Roda *et al.* 1995). However, the zoning in the dravite crystals described here is characterized by higher ^{Y+Z}Al and X-site vacancies in the inner zones, in contrast to the outer zones, which have higher Fe, Mg, Ti, Na, and Ca contents (Fig. 3); moreover, restricted variations in Fe/Mg were observed (Fig. 4).

The foitite–schorl crystals have high Fe contents (1.904–2.441 *apfu*), but low Mg contents (0.071–0.600 *apfu*). The ^{Y+Z}Al contents are in the range of 6.027 and 6.689 *apfu*. The Ti contents are lower than those in the dravite crystals (0.009 *apfu* on average). Sodium is the principal cation at the X site (0.349–0.618 *apfu*); Ca

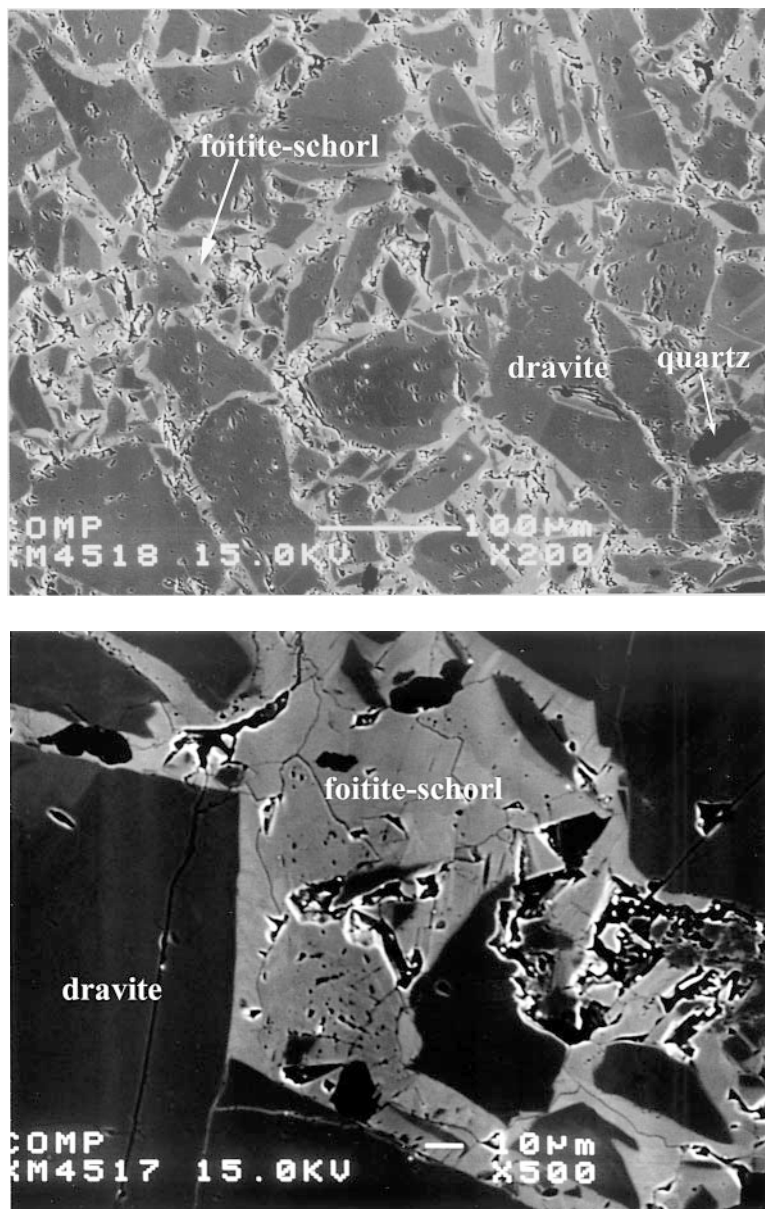


FIG. 1. BSE images of tourmaline crystals in the endocontact zone. a) The euhedral dravite crystals are simply zoned, and the rim zones are lighter than the cores. The anhedral foitite-schorl crystals fill the interstices of euhedral crystals of dravite. b) The foitite-schorl crystal is slightly heterogeneous.

contents are very low (0–0.093 *apfu*). Consequently, the occupancy of the *X* site shows a variable trend, and the calculated *X*-site vacancies range from 0.315 to 0.626 *apfu*, indicating a continuous variation between schorl and foitite (Figs. 3, 4). It is noteworthy that the crystals

with foitite as the dominant component exhibit Mg-enrichment, up to 0.46 *apfu*, similar to that reported in the literature (*e.g.*, 0.33 *apfu*: Francis *et al.* 1999, 0.58 *apfu*: Medaris *et al.* 2003), which may be related to the Mg-rich country rock. Minor elements such as Mn, Zn and

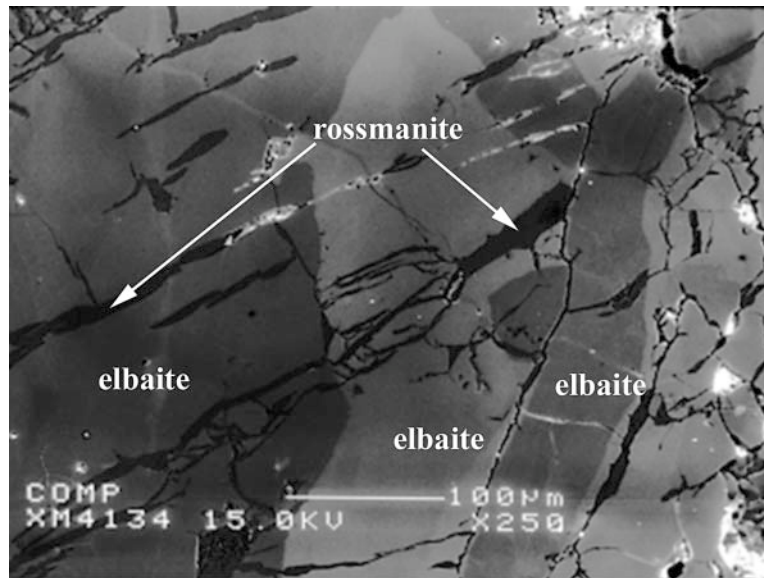


FIG. 2. BSE image of the host elbaite crystal and the cross-cutting vein-like rossmanite crystals in the “cleavelandite – spodumene” zone.

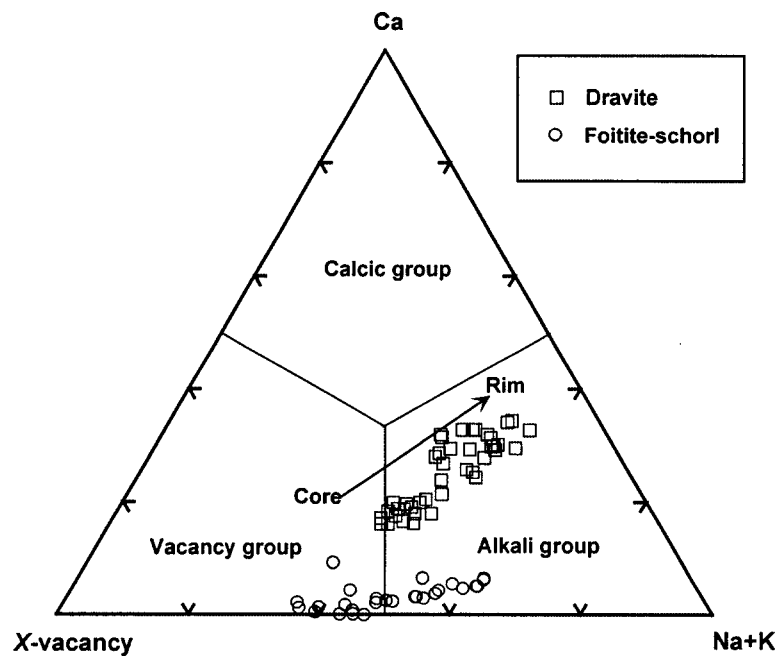


FIG. 3. The classification of tourmaline present in the endocontact zone.

K, both in the dravite crystals and in the foitite-schorl crystals, exhibit no obvious trends in variation.

*Elbaite and rossmanite
in the "cleavelandite" – spodumene zone*

Forty-seven point-analyses on the elbaite and rossmanite crystals were done. Representative compositions are given in Table 3. The host elbaite crystals are relatively $Y+Z$ Al-poor (7.137–7.681 *apfu*), whereas Li and Mn are relatively enriched (1.080–1.423 *apfu* and 0.087–0.261 *apfu*, respectively). The X-site cations of elbaite are dominated by Na (0.484–0.712 *apfu*), with subordinate Ca (0.043–0.127 *apfu*) (Fig. 5). The occupancy of the site is variable, indicating the existence of the rossmanite component, with the calculated values of X-site vacancy ranging from 0.225 to 0.449 *apfu*. Corresponding to the relative gray levels of the elbaite crystals in BSE (Fig. 2), the lighter areas have distinctly

higher Fe and Mn contents, whereas the darker areas are higher in Al and Li.

In the rossmanite crystals, $Y+Z$ Al is distinctly high (7.833–7.987 *apfu*) in contrast to Li and Mn (0.905–1.051 *apfu* and 0–0.010 *apfu*, respectively), and very low Na + Ca contents (Na: 0–0.069 *apfu*; Ca: 0–0.013 *apfu*) suggest the presence of a significant vacancy at this site (>0.930 *apfu*), indicating a large proportion of the rossmanite component. One analysis with the X-site vacancy value of about 1.000 *apfu* reveals it to be nearly pure rossmanite. This proportion of the vacancy is distinctly higher than that described in rossmanite from the type locality (0.57 *apfu*) (Selway *et al.* 1998), and it represents the most strongly vacancy-dominant variety recorded to date. Trace-element concentrations (such as Ti, Mg, Zn, and K) are close to the detection limits in both kinds of tourmaline crystals, and display no obvious correlations with the extent of the X-site vacancy.

TABLE 2. SELECTED EPMA RESULTS OF DRAVITE AND FOITITE-SCHORL IN THE ENDOCONTACT ZONE, KOKTOKAY No. 3 GRANITIC PEGMATITE DYKE, ALTAI, NW CHINA

	Dravite1		Dravite2		Foitite-schorl			
	core	rim	core**	rim	1	2	3	4
SiO ₂ wt.%	36.94	36.02	35.71	35.63	35.41	35.85	35.48	35.14
TiO ₂	0.12	0.57	0.18	0.56	0.02	0.04	0.01	0.23
Al ₂ O ₃	32.46	30.33	32.68	30.37	34.32	33.09	32.52	31.74
FeO	6.45	7.48	6.51	7.60	14.76	13.69	14.82	15.13
MgO	7.18	7.96	7.36	8.37	0.78	1.84	0.78	1.53
MnO	–	0.06	0.08	–	0.27	0.23	0.26	0.28
ZnO	0.07	–	–	–	0.05	0.03	0.05	0.09
CaO	0.93	1.58	0.91	1.66	0.07	–	0.18	0.29
Na ₂ O	1.46	1.34	1.28	1.41	1.11	1.41	1.60	1.86
K ₂ O	0.01	0.03	0.02	–	0.01	0.05	0.01	0.02
H ₂ O*	3.67	3.52	3.63	3.49	3.58	3.58	3.54	3.43
Li ₂ O*	0.19	0.02	0.00	0.00	0.01	0.07	0.23	0.10
B ₂ O ₃ *	10.67	10.48	10.51	10.48	10.39	10.37	10.25	10.24
F	0.03	0.20	–	0.27	–	–	–	0.21
–O=F	0.01	0.08	–	0.11	–	–	–	0.09
Total	100.17	99.51	98.87	99.73	100.78	100.25	99.73	100.20
Si <i>apfu</i>	6.018	5.973	5.904	5.907	5.923	6.008	6.016	5.966
^Y Al	0.000	0.027	0.096	0.093	0.077	0.000	0.000	0.034
Ti	0.015	0.071	0.022	0.070	0.003	0.005	0.001	0.029
^{Y+Z} Al	6.232	5.901	6.272	5.841	6.689	6.535	6.499	6.318
Fe	0.879	1.037	0.900	1.054	2.065	1.919	2.101	2.148
Mg	1.744	1.968	1.814	2.069	0.195	0.460	0.197	0.387
Mn	–	0.008	0.011	–	0.038	0.033	0.037	0.040
Zn	0.008	–	–	–	0.006	0.004	0.006	0.011
Li	0.122	0.015	0.000	0.000	0.005	0.045	0.158	0.065
Ca	0.162	0.281	0.161	0.295	0.013	–	0.033	0.053
Na	0.461	0.431	0.410	0.453	0.360	0.458	0.526	0.612
K	0.002	0.006	0.004	–	0.002	0.011	0.002	0.004
□	0.375	0.282	0.425	0.252	0.625	0.531	0.439	0.331
F	0.015	0.105	–	0.142	–	–	–	0.113
OH	3.985	3.895	4.000	3.858	4.000	4.000	4.000	3.887

* Calculated from stoichiometry (see explanation in the text); ^YAl and ^{Y+Z}Al denote the Al contents at the Y and Y + Z sites, respectively. –: below detection limits; □: vacancy at the X site. **: Magnesianfoitite–dravite. The structural formula is calculated on the basis of 31 anions.

TABLE 3. SELECTED EPMA RESULTS OF ELBAITE AND ROSSMANITE IN THE "CLEAVELANDITE" – SPODUMENE ZONE, KOKTOKAY No. 3 GRANITIC PEGMATITE DYKE, ALTAI, NW CHINA

	Elbaite				Rossmanite				
	1	2	3	4	1	2	3	4	5*
SiO ₂ wt.%	37.80	38.35	37.23	38.11	38.17	38.36	37.43	39.08	38.10
TiO ₂	–	–	–	0.02	–	–	0.01	–	–
Al ₂ O ₃	39.76	42.93	40.04	41.68	44.32	43.84	42.17	43.40	44.60
FeO	1.34	0.22	1.55	0.25	0.63	0.69	0.90	0.55	–
MgO	–	0.02	–	–	–	0.03	–	0.03	–
MnO	1.42	0.67	1.54	0.77	0.07	0.01	0.03	–	–
ZnO	0.27	0.11	0.41	–	0.20	0.28	0.09	0.10	–
CaO	0.37	0.33	0.39	0.35	0.04	0.08	0.01	–	–
Na ₂ O	1.97	1.67	2.08	1.74	0.02	0.13	0.22	–	1.43
K ₂ O	–	–	–	0.03	0.02	0.01	–	–	–
H ₂ O*	3.71	3.81	3.69	3.81	3.84	3.83	3.66	3.72	3.70
Li ₂ O*	1.83	1.92	1.75	1.97	1.46	1.51	1.49	1.64	1.13
B ₂ O ₃ *	10.95	11.30	10.93	11.13	11.24	11.23	10.89	11.26	10.88
F	0.15	0.19	0.17	0.05	0.09	0.10	0.21	0.35	0.20
–O=F	0.06	0.08	0.07	0.02	0.04	0.04	0.09	0.15	0.08
Total	99.51	101.44	99.71	99.89	100.06	100.06	97.02	99.98	99.96
Si <i>apfu</i>	5.998	5.899	5.919	5.953	5.903	5.937	5.975	6.031	5.92
^Y Al	0.002	0.101	0.081	0.047	0.097	0.063	0.025	0.000	–
Ti	–	–	–	0.002	–	–	0.001	–	–
^{Y+Z} Al	7.434	7.681	7.422	7.627	7.981	7.933	7.908	7.894	8.17
Fe	0.178	0.028	0.206	0.033	0.081	0.089	0.120	0.071	–
Mg	–	–	–	0.006	0.004	0.002	–	–	–
Mn	0.191	0.087	0.207	0.102	0.009	0.001	0.004	–	–
Zn	0.032	0.012	0.048	–	0.023	0.032	0.011	0.011	–
Li	1.165	1.186	1.116	1.236	0.906	0.937	0.956	1.017	–
Ca	0.063	0.054	0.066	0.059	0.007	0.013	0.002	–	–
Na	0.606	0.498	0.641	0.527	0.006	0.039	0.068	–	0.43
K	–	–	–	0.006	0.004	0.002	–	–	–
□	0.331	0.448	0.293	0.408	0.983	0.946	0.930	1.000	0.57
F	0.075	0.092	0.085	0.025	0.044	0.049	0.106	0.171	0.10
OH	3.925	3.908	3.915	3.975	3.956	3.951	3.894	3.829	3.83

* calculated from stoichiometry (see explanation in the text); ^YAl and ^{Y+Z}Al denote the Al contents at the Y and Y + Z sites, respectively. –: below detection limits; □: vacancy at the X site. * from Selway *et al.* (1998). The structural formula is calculated on the basis of 31 anions.

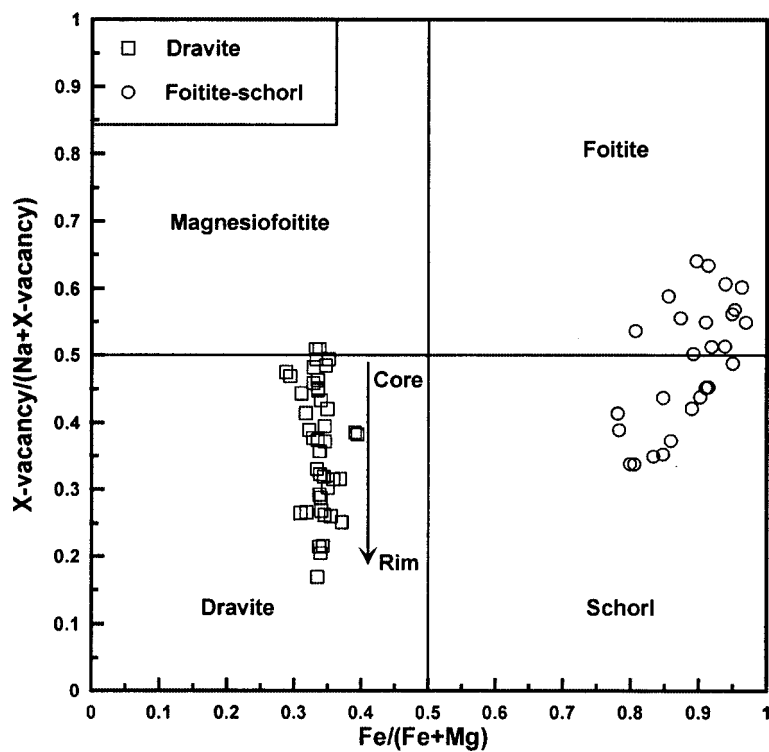


FIG. 4. Nomenclature diagram for tourmaline present in the endocontact zone.

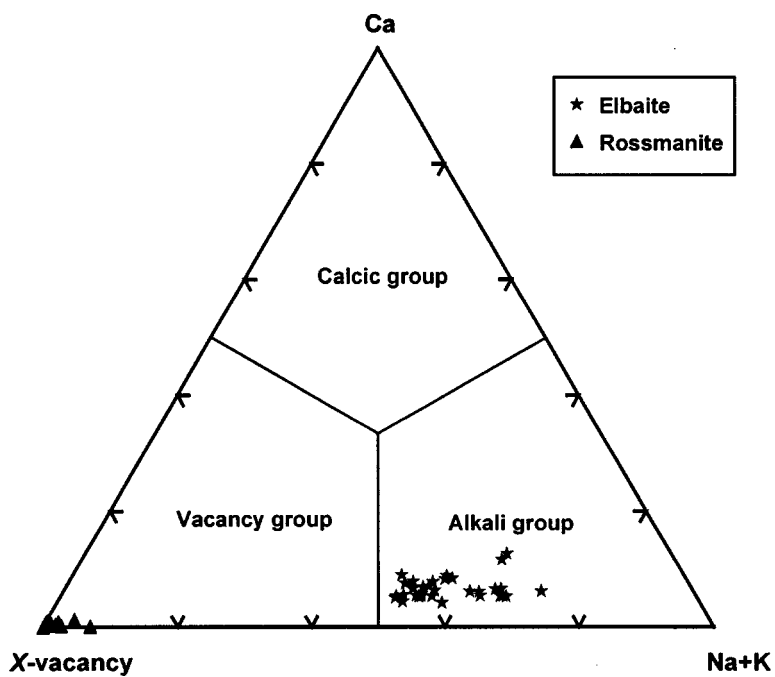


FIG. 5. The classification of tourmaline in the "cleavelandite" - spodumene zone.

DISCUSSION

Compositional variations of tourmaline in the endocontact zone

Textural relations reveal that the evolution of tourmaline in the endocontact zone can be divided in two stages: the euhedral to anhedral crystals of dravite and the anhedral foitite–schorl crystals filling interstices (Figs. 1a, b). Relative to the earlier Mg-dominant tourmaline (dravite) crystals, the later Fe-dominant tourmaline (foitite–schorl) crystals are distinctly higher in Fe,

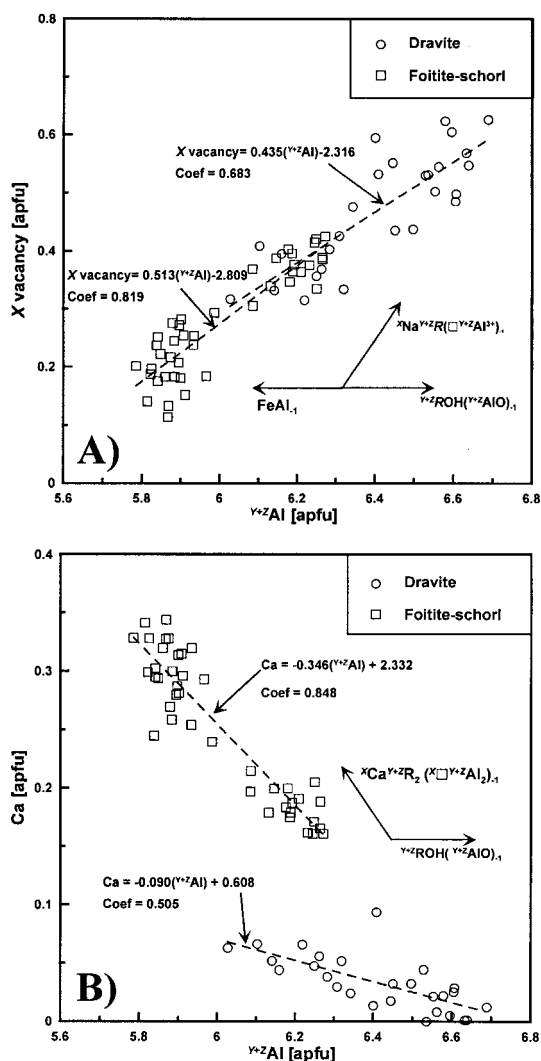


FIG. 6. $Y+ZAl$ versus A) X vacancy and B) Ca in the tourmaline of the endocontact zone. The dashed lines are the best fits to the data points.

Al, and X-site vacancy, and more depleted in Mg, Ca, and Na. The earlier Mg-dominant tourmaline crystals display increasing core-to-rim contents of Fe, Mg, Ti at the Y + Z sites (Table 2) and Ca, Na at the X site (Table 2, Fig. 3) at the expense of $Y+ZAl$ and X-site vacancy. In contrast to obvious variations recorded in the literature (e.g., Roda *et al.* 1995), the Fe:Mg ratio from core to rim in the zoned dravite crystals displays restricted variations (Fig. 4). Thus, with increasing evolution of single crystals, the dravite component became enriched in contrast to the magnesiofoitite component (Fig. 4). The evolution characteristics of the Fe:Mg ratios may reflect the parallel variations of their bulk concentrations in the host systems. The Fe-dominant tourmaline crystals also display large compositional variations, though this has not been demonstrated in BSE images. The contents of Fe, Mg, $Y+ZAl$, Na, and X-site vacancy display obvious variations, reflecting competitions between foitite and schorl end-member components.

Corresponding to the compositional variations of tourmaline in the endocontact zone, the chemical changes from Mg-dominant tourmaline to Fe-dominant tourmaline are most likely expressed by the substitution mechanisms: $Fe(Mg)_{-1}$, ${}^XNa^{Y+Z}R({}^X\Box^{Y+Z}Al)_{-1}$, and ${}^XCa^{Y+Z}R_2({}^X\Box^{Y+Z}Al_2)_{-1}$, where $Y+ZR = Fe_{tot} + Mg + Mn + Zn$ (cf. Novák & Taylor 2000). The element exchanges in the zoned Mg-dominant tourmaline crystals mainly involve Ca, Na, vacancy at the X site (Figs. 3, 4) and $Y+ZR$ and $Y+ZAl$ at the Y + Z sites (Fig. 6a); moreover, the variations in the Fe:Mg ratio are very restricted. The compositional variations are most consistent with the following substitutions: ${}^XNa^{Y+Z}R({}^X\Box^{Y+Z}Al)_{-1}$ and ${}^{Y+Z}ROH({}^{Y+Z}AlO)_{-1}$ (Fig. 6a) (cf. Henry *et al.* 2002), with ${}^XCa^{Y+Z}R_2({}^X\Box^{Y+Z}Al_2)_{-1}$ (Fig. 6b). On the other hand, the content of Ca is low, and the compositional variations of the Fe-dominant tourmaline crystals mainly involve the variations of Na, X-site vacancy, $Y+ZR$, and $Y+ZAl$; moreover, the Fe:Mg ratio also displays large variations (Fig. 4). Therefore, the major substitutions in the Fe-dominant tourmaline crystals would seem to be: $Fe(Mg)_{-1}$, ${}^XNa^{Y+Z}R({}^X\Box^{Y+Z}Al)_{-1}$, ${}^{Y+Z}ROH({}^{Y+Z}AlO)_{-1}$ (Fig. 6a) (cf. Henry *et al.* 2002), combined with minor ${}^XCa^{Y+Z}R_2({}^X\Box^{Y+Z}Al_2)_{-1}$ (Fig. 6b), mainly reflecting variations between schorl and foitite components (Fig. 4).

Compositional variations of tourmaline in the "cleavelandite" – spodumene zone

Relative to foitite, rossmanite is only described from the type locality (Selway *et al.* 1998). Therefore, the substitution mechanism involved in producing rossmanite is seldom discussed. However, Selway *et al.* suggested that rossmanite could be derived from elbaite by the substitution ${}^XNa_2{}^YLi({}^X\Box_2{}^YAl)_{-1}$.

In the tourmaline crystals from the "cleavelandite" – spodumene zone, an obvious compositional gap can be recognized (Figs. 5, 7), and the rossmanite crystals are markedly richer in $Y+ZAl$ and X-site vacancy than the

host crystals of elbaite, with lower Na, Ca, Mn, and Li (Figs. 5, 7, Table 3). The average Fe content of the rossmanite crystals (0.080 *apfu*) is slightly lower than that of the host elbaite crystals (0.099 *apfu*). Similarly in the endocontact zone, the evolution of tourmaline in the “cleavelandite” – spodumene zone can be considered in two stages, corresponding to the developments of elbaite and rossmanite. The compositional changes from the host elbaite crystals to the veinlet rossmanite crystals are mostly likely explained by the substitutions: ${}^X\text{Na}^Y(\text{Mn,Fe})({}^X\Box^Y\text{Al})_{-1}$ and ${}^X\text{Na}_2^Y\text{Li}({}^X\Box^Y\text{Al})_{-1}$. In the first stage, the compositional variations of the host elbaite crystals principally involve Na, X-site vacancy, ${}^{Y+Z}\text{Al}$, Mn, and Fe (Figs. 5, 7, Table 3), which can be expressed by the substitution ${}^X\Box^Y\text{Al}[{}^X\text{Na}^Y(\text{Fe,Mn})]_{-1}$, which reflects the variations between rossmanite and schorl components. However, in the second stage, there is a slight variation in ${}^{Y+Z}\text{Al}$ and Li in the veinlet rossmanite crystals. The compositional variation most likely involve the substitution ${}^Y\text{AlO}_2({}^Y\text{Li}(\text{OH})_2)_{-1}$ (cf. Novák & Taylor 2000), reflecting the variations between elbaite and an “oxy-Al-tourmaline” component.

Formation of foitite and rossmanite

In the Koktokay No. 3 granitic pegmatite dyke, tourmaline occurs both in the contact zone and in most of the internal textural zones. However, the X-site-vacant tourmaline crystals are restricted to the endocontact zone and the “cleavelandite” – spodumene zone only. The relatively localized occurrences suggests that they formed under different physicochemical conditions than the common alkali or calcic tourmaline.

Textural relations showing that foitite–schorl filled the interstices among dravite crystals at least reveal that late formation of foitite–schorl must be due to the influx of hydrothermal fluids. The distinct compositional gap between dravite and foitite–schorl also indicates different physicochemical conditions during early and late stages of the tourmaline precipitation in the endocontact zone, although high activities of Fe and B are maintained throughout the process. Factors controlling the stability of dravite in the endocontact zone include: (1) the abundance of Mg (and also Fe) produced by the breakdown of pyroxene + biotite, and of Ca, Na by the breakdown of plagioclase of the country rock (metagabbro), and (2) an influx of B, Al and F from the pegmatite-derived fluids. In contrast to dravite, foitite–schorl is distinctly Mg- and Ca-depleted, indicating that Fe is unlikely to have been derived from the Mg- and Ca-rich metagabbro. Thus, a pegmatite source of Fe in foitite–schorl is considered likely. The formation of X-site-vacant tourmaline is generally related to a lack of Na or Ca in the systems (Wodara & Schreyer 2000, Medaris *et al.* 2003). Synthesis experiments (von Goerne & Franz 2000, von Goerne *et al.* 2001) also suggest that the amount of X-site vacancy depends strongly on the bulk concentrations of Na and Ca in the

system in which tourmalines crystallize, as well as temperature. Therefore, for the foitite–schorl in this study, the significant X-site vacancy may be attributed to depletion in Na and Ca in the reactive fluids. The core-to-rim compositional variations in the dravite crystals record the variation in alkali concentration in the dravite-growing systems (Medaris *et al.* 2003), whereas the compositional heterogeneity of foitite–schorl may reflect the locally variable concentrations of the alkalis in the reactive fluids.

In the “cleavelandite” – spodumene zone, rossmanite appears typically as veinlets in the host crystals of elbaite. This textural feature may indicate that rossmanite and elbaite formed in different systems, and rossmanite developed from the hydrothermal fluids filling the fractures of the host elbaite crystals (cf. Henry *et al.* 2002). In composition, the rossmanite crystals in the veinlets display a distinct gap with the host crystals of elbaite, and the former is characterized by elevated X-site vacancies (>0.930 *apfu*). As mentioned above, X-site-vacant tourmalines, including rossmanite, should be products of crystallization in a Na–Ca-poor system. Further, von Goerne *et al.* (2001) indicated that Na-rich

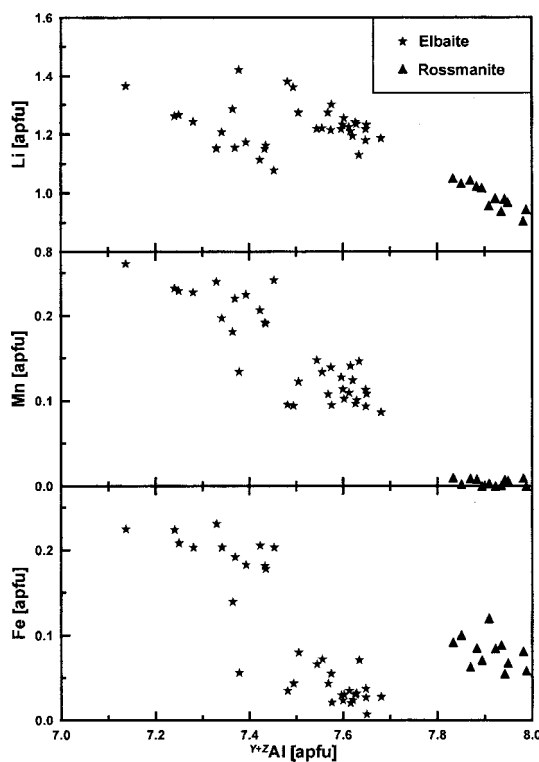


Fig. 7. Covariations of ${}^{Y+Z}\text{Al}$ versus Li, Mn, and Fe for tourmaline in the “cleavelandite” – spodumene zone.

phases (such as albite) might perturb the distribution of Na in the structure of tourmaline; however, the buffering effect is unlikely to promote the formation of near-end-member rossmanite (*cf.* von Goerne *et al.* 2001). Thus, the significant X-site vacancy in elbaite may be caused by the buffering effect of a Na-rich phase (such as albite), whereas the elevated X-site vacancy must be the result of a local lack of Na and Ca in the hydrothermal fluids.

ACKNOWLEDGEMENTS

This work was financially supported by the National Natural Science Foundation of China (grants 40025209 and 40221301). We thank Carl A. Francis, Darrell J. Henry for their critical reviews, and Robert F. Martin and Franklin F. Foit, Jr., for editorial handling of the manuscript.

REFERENCES

- AURISICCHIO, C., OTTOLINI, L. & PEZZOTTA, F. (1999): Electron- and ion-microprobe analyses, and genetic inferences of tourmalines of the foitite-schorl solid solution, Elba Island (Italy). *Eur. J. Mineral.* **11**, 217-225.
- ČERNÝ, P. (1991): Rare-element granitic pegmatites. I. Anatomy and internal evolution of pegmatite deposits. *Geosci. Canada* **18**, 49-67.
- CHEN FUWEN, LI HUAQIN, WANG DENGHONG, CAI HONG & CHEN WEN (2000): New chronological evidence for Yanshanian diagenetic mineralization in China's Altay orogenic belt. *Chin. Sci. Bull.* **45**, 108-114.
- DUTROW, B.L. & HENRY, D.J. (2000): Complexly zoned fibrous tourmaline, Cruzeiro mine, Minas Gerais, Brazil: a record of evolving magmatic and hydrothermal fluids. *Can. Mineral.* **38**, 131-143.
- FOIT, F.F., JR., FUCHS, Y. & MYERS, P.E. (1989): Chemistry of alkali-deficient schorls from two tourmaline-dumortierite deposits. *Am. Mineral.* **74**, 1317-1324.
- FRANCIS, C.A., DYAR, M.D., WILLIAMS, M.L. & HUGHES, J.M. (1999): The occurrence and crystal structure of foitite from a tungsten-bearing vein at Copper Mountain, Taos County, New Mexico. *Can. Mineral.* **37**, 1431-1438.
- HAWTHORNE, F.C. & HENRY, D.J. (1999): Classification of the minerals of the tourmaline group. *Eur. J. Mineral.* **11**, 201-215.
- _____, SELWAY, J.B., KATO, A., MATSUBARA, S., SHIMIZU, M., GRICE, J.D. & VAJDAK, J. (1999): Magnesiofoitite, $\square\text{Mg}_2\text{Al}\text{Al}_6(\text{Si}_6\text{O}_{18})(\text{BO}_3)_3(\text{OH})_4$, a new alkali-deficient tourmaline. *Can. Mineral.* **37**, 1439-1443.
- HENRY, D.J., DUTROW, B.L. & SELVERSTONE, J. (2002): Compositional asymmetry in replacement tourmaline – an example from the Tauern Window, Eastern Alps. *Geol. Mater. Res.* **4**, 1-18.
- JIANG, SHAO-YONG, PALMER, M.R. & SLACK, J.F. (1997): Alkali-deficient tourmaline from the Sullivan Pb-Zn-Ag deposit, British Columbia. *Mineral. Mag.* **61**, 853-860.
- MACDONALD, D.J., HAWTHORNE, F.C. & GRICE, J.D. (1993): Foitite, $\square\text{Fe}^{2+}_2(\text{Al,Fe}^{3+})\text{Al}_6\text{Si}_6\text{O}_{18}(\text{BO}_3)_3(\text{OH})_4$, a new alkali-deficient tourmaline: description and crystal structure. *Am. Mineral.* **78**, 1299-1303.
- MEDARIS, L.G., JR., FOURNELLE, J.H. & HENRY, D.J. (2003): Tourmaline-bearing quartz veins in the Baraboo quartzite, Wisconsin: occurrence and significance of foitite and "oxyfoitite". *Can. Mineral.* **41**, 749-758.
- NOVÁK, M. & TAYLOR, M.C. (2000): Foitite: formation during late stages of evolution of complex granitic pegmatites at Dobra Voda, Czech Republic, and Pala, California, U.S.A. *Can. Mineral.* **38**, 1399-1408.
- PEZZOTTA, F., HAWTHORNE, F.C., COOPER, M.A. & TEERTSTRA, D.K. (1996): Fibrous foitite from San Piero in Campo, Elba, Italy. *Can. Mineral.* **34**, 741-744.
- RODA, E., PESQUERA, A. & VELASCO, F. (1995): Tourmaline in granitic pegmatites and their country rocks, Fregeneda area, Salamanca, Spain. *Can. Mineral.* **33**, 835-848.
- SELWAY, J.B., NOVÁK, M., HAWTHORNE, F.C., ČERNÝ, P., OTTOLINI, L. & KYSER, T.K. (1998): Rossmanite, $\square(\text{LiAl}_2)\text{Al}_6(\text{Si}_6\text{O}_{18})(\text{BO}_3)_3(\text{OH})_4$, a new alkali-deficient tourmaline: description and crystal structure. *Am. Mineral.* **83**, 896-900.
- VON GOERNE, G. & FRANZ, G. (2000): Synthesis of Ca-tourmaline in the system $\text{CaO-MgO-Al}_2\text{O}_3\text{-SiO}_2\text{-B}_2\text{O}_3\text{-H}_2\text{O-HCl}$. *Mineral. Petrol.* **69**, 161-182.
- _____, _____ & HEINRICH, W. (2001): Synthesis of tourmaline solid solutions in the system $\text{Na}_2\text{O-MgO-Al}_2\text{O}_3\text{-SiO}_2\text{-B}_2\text{O}_3\text{-H}_2\text{O-HCl}$ and the distribution of Na between tourmaline and fluid at 300 to 700°C and 200 MPa. *Contrib. Mineral. Petrol.* **141**, 160-173.
- WANG, X.J., ZOU, T.R., XU, J.G., YU, X.Y. & QIU, Y.Z. (1981): *Study of Pegmatite Minerals of the Altai Region*. Science Publishing House, Beijing, China.
- WODARA, U. & SCHREYER, W. (2001): X-site vacant Al-tourmaline: a new synthetic end-member. *Eur. J. Mineral.* **13**, 521-532.
- ZHANG, A.C., WANG, A.C., HU, H., ZHANG, H., ZHU, J.C. & CHEN, X.M. (2004): Chemical evolution of Nb-Ta oxides and zircon from the Koktokay No.3 granitic pegmatite dyke, Altai, northwestern China. *Mineral. Mag.* (in press).
- ZHU, J.C., WU, C.N., LIU, C.S., LI, F.C., HUANG, X.L. & ZHOU, D.S. (2000): Magmatic-hydrothermal evolution and genesis of Koktokay No.3 rare metal pegmatite dyke, Altai, China. *Geol. J. China Univ.* **6**, 40-52 (in Chinese, with English abstr.).

Received September 28, 2003, revised manuscript accepted April 12, 2004.